

Modeling the effect of sleep regulation on a neural mass model

Michael Schellenberger Costa¹ · Jan Born² · Jens Christian Claussen³ · Thomas Martinetz¹

Received: 25 September 2015 / Revised: 9 March 2016 / Accepted: 11 March 2016 / Published online: 11 April 2016
© Springer Science+Business Media New York 2016

Abstract In mammals, sleep is categorized by two main sleep stages, rapid eye movement (REM) and non-REM (NREM) sleep that are known to fulfill different functional roles, the most notable being the consolidation of memory. While REM sleep is characterized by brain activity similar to wakefulness, the EEG activity changes drastically with the emergence of K-complexes, sleep spindles and slow oscillations during NREM sleep. These changes are regulated by circadian and ultradian rhythms, which emerge from an intricate interplay between multiple neuronal populations in the brainstem, forebrain and hypothalamus and the resulting varying levels of neuromodulators. Recently, there

has been progress in the understanding of those rhythms both from a physiological as well as theoretical perspective. However, how these neuromodulators affect the generation of the different EEG patterns and their temporal dynamics is poorly understood. Here, we build upon previous work on a neural mass model of the sleeping cortex and investigate the effect of those neuromodulators on the dynamics of the cortex and the corresponding transition between wakefulness and the different sleep stages. We show that our simplified model is sufficient to generate the essential features of human EEG over a full day. This approach builds a bridge between sleep regulatory networks and EEG generating neural mass models and provides a valuable tool for model validation.

Action Editor: Michael Breakspear

Jens Christian Claussen and Thomas Martinetz contributed equally

✉ Michael Schellenberger Costa
schellenberger@inb.uni-luebeck.de

Jan Born
jan.born@uni-tuebingen.de

Jens Christian Claussen
j.claussen@jacobs-university.de

Thomas Martinetz
martinetz@inb.uni-luebeck.de

¹ Institute for Neuro and Bioinformatics, University of Lübeck, Ratzeburger Allee 160, 23538 Lübeck, Germany

² Institute for Medical Psychology and Behavioural Neurobiology, University of Tübingen, Otfried-Müller-Str. 25, 72076 Tübingen, Germany

³ Life Sciences, Chemistry, Jacobs University Bremen, Campus Ring 1, 28759 Bremen, Germany

Keywords Neural mass · EEG · Sleep regulation · Neuromodulators · Sleep · Sleep rhythms

1 Introduction

During sleep, the brain alternates between two core sleep stages: rapid-eye-movement (REM) and non-REM (NREM) sleep (Fig. 1), the latter being predominant during early sleep while decreasing in duration during the night and vice versa. NREM sleep is further subdivided into sleep stages N1-N3, that are dominated by low-frequency high-amplitude oscillations in the electroencephalogram (EEG). Sleep stage N2 as a lighter form of non-REM sleep is hallmarked by the occurrence of sleep spindles and K-complexes (KCs), whereas deeper N3 sleep is dominated by slow wave activity (SWA) (Iber et al. 2007). In contrast, REM sleep exhibits low amplitude activity of higher frequency, which resembles the EEG found during wakefulness (Rasch and Born 2013).

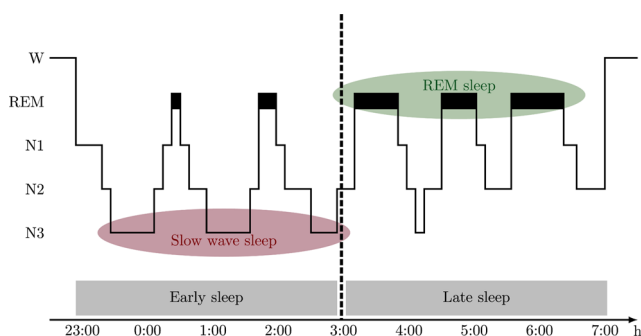


Fig. 1 Typical human sleep profile This picture depicts a typical hypnogram during a night. The early night is dominated by NREM sleep, that is further subdivided into sleep stages N1–N3, whereas REM sleep prevails during the second half (late sleep). During NREM sleep, cholinergic activity is at a minimum, while REM sleep shows similar or even higher levels than wakefulness. Aminergic activity is high during waking, intermediate during SWS, and minimal during REM sleep. Modified from Rasch and Born (Rasch and Born 2013)

The EEG as a macroscopic quantity is generated by the activity of neurons in different areas of the brain. For detailed single neuron approaches such as the classical Hodgkin-Huxley models such large scale simulations are challenging due to their complexity and the resulting computational load. Here, neural mass models pioneered by the work of Wilson and Lopez da Silva (Wilson and Cowan 1973; Lopes da Silva et al. 1974), have shown great success generating rhythms present in the wake EEG, as well as evoked responses (Jansen et al. 1993; Wendling et al. 2002; David and Friston 2003). Rather than considering individual neurons, they describe the dynamics of a neural population through an averaged representation of that specific cell type, which relates directly to mesoscopic measurements like the EEG (Coombes 2005; Deco et al. 2008).

Recently, we could demonstrate that a neural mass model of the cortex, extended by an additive activity-dependent feedback current, is able to generate the EEG signal of sleep stages N2 and N3 (Weigenand et al. 2014). Based upon a bifurcation analysis, we found two key parameters, neural gain $1/\sigma_p$ and the strength of pyramidal firing rate adaptation g_{KNa} , to be responsible for the transition between wakefulness and the different NREM sleep stages. Importantly, both bifurcation parameters are known to be affected by neuromodulators. Application of acetylcholine blocks potassium currents (McCormick 1989; McCormick and Huguenard 1992), such as I_{KNa} , whereas they are activated by GABA. Furthermore, the neural gain is modulated by acetylcholine (Disney et al. 2007; Gullledge et al. 2009; Soma and Shimegi 2016), serotonin (Zhang and Arsenault 2005), and noradrenalin (McCormick 1989; Timmons et al. 2004), with those levels changing in specific patterns throughout the sleep-wake cycle (Léna et al. 2005).

The transition between wakefulness and the sleep stages and therewith the corresponding levels of neuromodulators (Lydic and Baghdoyan 2005), is coordinated by the activity of neuronal populations distributed in different brain areas, primarily the forebrain, brainstem and hypothalamus (Moruzzi 1972; Saper et al. 2005). Depending on the participating neuromodulators and brain structures and due to their specific temporal dynamic there is a differentiation between a wake-NREM switch and REM-NREM cycling, respectively (Booth and Diniz Behn 2014). The wake-NREM switch has been successfully described by the two-process model, which is based on a homeostatic sleep drive (Borbély 1982; Daan et al. 1984) or more specifically mutual inhibition between wake-promoting (locus coeruleus (LC), dorsal raphe nucleus (DR)) and sleep-promoting populations (ventrolateral preoptic nucleus (VLPO)) (Saper et al. 2001; Diniz Behn and Booth 2010). Additionally, the sleep wake transition is heavily influenced by the circadian rhythm, which is mainly acting through the suprachiasmatic nucleus (SCN).

The activity of those populations is closely related to the levels of the neurotransmitter noradrenalin and serotonin. The NREM-REM cycling has originally been assumed to be driven by reciprocal interaction between cholinergic REM promoting and aminergic wake promoting REM-on populations (McCarley and Hobson 1975; Luppi et al. 2006; Datta and MacLean 2007). However, recent research indicates an involvement of GABAergic populations in the regulation of REM sleep (Lu et al. 2006; Fuller et al. 2007; Brown et al. 2008), that also involve mutual inhibition. Additionally, the NREM-REM rhythm is affected by orexinergic neurons located in the perifornical area (Peyron et al. 1998).

Early approaches on modeling the sleep-wake transition focused on homeostatic regulation (Borbély 1982; Forger et al. 1999). Only recently the faster cycling between NREM and REM sleep has been incorporated with varying levels of anatomical detail (Tamakawa et al. 2006; Diniz Behn et al. 2007; Phillips and Robinson 2007; Diniz Behn and Booth 2010; Rempe et al. 2009; Kumar et al. 2012). These models describe the sleep-wake transition through firing rates of the involved neuronal populations. Depending on whether wake-promoting, REM-off or REM-on populations are active the system is assumed to be in a state of wakefulness, REM or NREM sleep. The transition between those stages is driven by synaptic interactions between the involved populations and the corresponding level of neurotransmitters, which is modulated by circadian and homeostatic drives. For the sake of simplicity we will restrict ourselves to a simplified model (Diniz Behn and Booth 2012), that accumulates populations which serve similar functionality into a single population neglecting more complex interactions (Rempe et al. 2009; Diniz Behn and Booth 2010; Kumar et al. 2012), including interactions with the

SCN and circadian modulation. This results in a simple model with only three populations (WAKE, NREM, and REM). See (Fleshner et al. 2011; Gleit et al. 2013) for extended models incorporating circadian modulation of the sleep regulatory network.

Here, we demonstrate that sleep regulatory networks and neural mass models of the sleep EEG can be combined, to provide a unified generating model of EEG activity for both wake and sleep. In addition to generating activity that closely resembles the EEG signals of the different sleep stages in humans, our model captures the ultradian cycling between NREM and REM sleep as well the transition between wakefulness and sleep. This approach enables us to infer activity within the sleep regulatory network from the EEG activity and vice versa, providing a useful tool for model validation.

2 Methods

In the following section, we briefly describe the neural mass formalism and our previous work on modeling the sleep EEG (Weigenand et al. 2014). Afterwards, we introduce the model of Diniz Behn and Booth (Diniz Behn and Booth 2012) of a sleep regulatory network and define the relation between the concentration of the neuromodulators and the bifurcation parameters of the cortical model. It is important to note, that while (Weigenand et al. 2014) and Diniz Behn and Booth (2012) are both firing rate models, they utilize slightly different formalisms.

2.1 Neural mass framework

The time course of a sufficiently large ensemble of individual neurons can be approximated by the evolution of the population average. Rather than considering the individual spikes, the averaged membrane voltage V_k of the neurons of population k is turned into a firing rate through a phenomenological firing rate function

$$Q_k(V_k) = \frac{Q_k^{\max}}{1 + \exp(-(V_k - \theta_k)/\sigma_k)}, \tag{1}$$

with maximal firing rate Q_k^{\max} , firing threshold θ_k and inverse neural gain σ_k . The firing rate function has a sigmoidal shape, which stems from the fluctuations of neuronal states or a distribution of thresholds in the population (Marreiros et al. 2008).

Spikes are generated at the soma and transmitted along the axons to the receiving population. For long range connections between different brain structures, delay plays an important role (Atay and Hutt 2006; Deco et al. 2009). As

intra-cortical connections are rather short and the sleep regulation acts on a slow timescale, we assume that the transmission is instantaneous and thereby neglect any delays. The postsynaptic response s_{mk} of synapse type m , which is either e for excitatory AMPA or g for inhibitory GABA synapses, on population k is then given by

$$\begin{aligned} s_{mk}(t) &= \sum_{k'} \alpha_m(t) \otimes N_{kk'} Q_{k'}(V_{k'}(t)), \\ &= \sum_{k'} \int_0^t \alpha_m(t - \tau) N_{kk'} Q_{k'}(V_{k'}(\tau)) d\tau. \end{aligned} \tag{2}$$

Here, the firing rate $Q_{k'}(V_{k'})$ of the presynaptic populations k' is scaled by a connectivity constant $N_{kk'}$, where k and k' can either be p for pyramidal or i for inhibitory populations. It is convoluted with the average synaptic response to a single spike

$$\alpha_m(t) = \gamma_m^2 t \exp(-\gamma_m t). \tag{3}$$

The rate constant γ_m defines the time course of the response of synapse type m . The evolution of the membrane voltage V_k is then given through summation of inputs from other populations as well as a passive leak current I_L ,

$$\begin{aligned} \tau_k \dot{V}_k &= -\bar{g}_L(V_k - E_L^k) \\ &\quad -\bar{g}_{\text{AMPA}} s_{ek}(V_k - E_{\text{AMPA}}) \\ &\quad -\bar{g}_{\text{GABA}} s_{gk}(V_k - E_{\text{GABA}}), \\ &= -I_L - I_{\text{AMPA}}(s_{ek}) - I_{\text{GABA}}(s_{gk}), \end{aligned} \tag{4}$$

Here, E denotes the Nernst potential, \bar{g} the maximal conductivity of the respective channel and τ_k the membrane time constant. The membrane potential is then again turned into an updated firing rate according to Eq. (1).

2.2 Sleeping cortex

To generate sleep EEG the basic neural mass framework is adapted as previously proposed in (Weigenand et al. 2014), such that it exhibits the key features of NREM sleep. It consists of a pyramidal (p) and an inhibitory (i) neural mass, that are coupled via AMPA and GABAergic synapses.

$$\begin{aligned} \tau_p \dot{V}_p &= I_L^p + I_{\text{AMPA}}(s_{ep}) + I_{\text{GABA}}(s_{gp}) - C_m^{-1} \tau_p I_{\text{KNa}}, \\ \tau_i \dot{V}_i &= I_L^i + I_{\text{AMPA}}(s_{ei}) + I_{\text{GABA}}(s_{gi}). \end{aligned} \tag{5}$$

In addition to the synaptic currents, the pyramidal population contains an activity dependent potassium current I_{KNa} , that is coupled via the membrane capacity C_m . This current acts as a slow, additive and activity-dependent firing rate adaptation, which is thought to be the main driver for the Up/Down state transition during NREM sleep

(Sanchez-Vives and McCormick 2000; Compte et al. 2003; Benita et al. 2012). It is implemented as

$$\begin{aligned} I_{\text{KNa}} &= g_{\text{KNa}} w_{\text{KNa}} ([\text{Na}]) (V_p - E_{\text{K}}), \\ \tau_{\text{Na}} [\dot{\text{Na}}] &= \alpha_{\text{Na}} Q_p - \text{Na}_{\text{pump}}([\text{Na}]). \end{aligned} \quad (6)$$

Please note that g_{KNa} is a dynamic variable, that depends on the maximal conductance \bar{g}_{KNa} and the concentration of the neuromodulators as defined by Eq. (11). The transition between wakefulness and the different NREM sleep stages is governed by the neural gain, $1/\sigma_p$ and adaptation strength g_{KNa} as previously described in Weigenand et al. (2014).

2.3 Sleep regulation

Rather than considering all neural populations involved in sleep regulation and their complex interaction (Rempe et al. 2009; Diniz Behn and Booth 2010; Kumar et al. 2012), we utilize a reduced sleep regulatory network, that merges neural populations with the same functionality into one of three types: wake-, NREM- and REM-promoting (Diniz Behn and Booth 2012). Each neuronal population is associated with a specific neurotransmitter. The wake-promoting neurons release noradrenalin, the NREM-promoting population acts through inhibitory GABA synapses and finally the REM-promoting population is linked to acetylcholine. This effectively reduces the sleep regulation to a twofold switch, between wakefulness-NREM and NREM-REM respectively.

In contrast to the model introduced in the previous section, Diniz Behn and Booth use a mathematically equivalent formulation, directly considering the firing rates $Q_k(V_k)$ rather than the membrane voltages V_k as their system variables (Diniz Behn et al. 2007; Diniz Behn and Booth 2010; 2012). To provide a direct link to their work, we will keep this formulation and denote the firing rate of population k as F_k for the sleep regulatory model. In the context of the sleep regulatory network k can either be W for the wake, N for the NREM, or R for the REM promoting population.

The firing rate F_k of the presynaptic population k elicits the release of neurotransmitters into the synaptic cleft. In their study on the reduced model, Diniz Behn and Booth assumed $\tau_k \gg \tau_X$, approximating the change in neurotransmitter concentration to be instantaneous. However, given that the time constants of the cortical model τ_p and τ_i are in the range of milliseconds, we cannot utilize this approximation. Consequently, the change of neurotransmitter concentration C_X is given by

$$\tau_X \dot{C}_X = \tanh(F_k/\gamma_X) - C_X. \quad (7)$$

Here, X depicts the type of neurotransmitter (i.e. E for noradrenalin, G for GABA or A for acetylcholine), γ_X the gain

of neurotransmitter release and τ_X the corresponding time constant.

Varying levels of neurotransmitters then change postsynaptic activity

$$\tau_k \dot{F}_k = Q_k^{SR} \left(\sum_X g_{X,k} C_X \right) - F_k, \quad (8)$$

with the time constant τ_k and weights $g_{X,k}$ that scale the strength of the synaptic responses. It is important to note, that due to the long timescale τ_k the synaptic inputs are assumed to act instantaneous. This is equivalent to Eq. (2) for $\alpha_m = \delta(t)$. The formulation of the firing rate function Q_k^{SR} utilized by Diniz Behn and Booth is mathematically equivalent to

$$Q_k^{SR}(Y) = \frac{F_k^{\max}}{1 + \exp(-(Y - \beta_k)/\alpha_k)}. \quad (9)$$

Here β_k denotes the firing rate threshold, α_k the corresponding inverse gain and Y the sum of the weighted neurotransmitter inputs. Note that for the NREM population the threshold is dependent on the homeostatic sleep drive h through $\beta_N = \kappa h$, where κ scales the influence of the sleep drive.

Following the two-process model originally proposed by Borbély (1982), the sleep-wake transition is driven by homeostatic sleep drive $h(t)$. It builds up during wakefulness, due to high activity F_W of the wake population and declines during sleep, when F_W is low. Assuming a maximal strength of h^{\max} , This can be described by

$$\dot{h} = \frac{h^{\max} - h}{\tau_h^w} \mathcal{H}(F_W - \theta_h) - \frac{h}{\tau_h^s} \mathcal{H}(\theta_h - F_W), \quad (10)$$

where \mathcal{H} stands for the Heaviside function, θ_h defines the sleep/wake transition threshold and τ_h^w and τ_h^s depict the time constants for increase and decline of h during wakefulness and sleep, respectively.

Please note that within the sleep regulatory network, noradrenalin, GABA, and acetylcholine act as *neurotransmitters*, i.e. they elicit a synaptic response. However, given the assumption that GABA from the sleep regulatory network is released on extrasynaptic sites in the cortex, they only *modulate* cortical dynamics. Therefore, whenever we are in the context of the cortical module, we refer to them as *neuromodulators*.

2.4 Action of neuromodulators

According to previous findings changes in the inverse neural gain σ_p and the adaptation strength g_{KNa} can lead to the transition between wakefulness and sleep stages N2/N3 (Weigenand et al. 2014). These parameters are known to be influenced by neuromodulators.

Acetylcholine blocks potassium currents (McCormick 1989; McCormick and Huguenard 1992), such as I_{KNa} and reduces firing rate adaptation of cortical neurons (Madison et al. 1987; Barkai and Hasselmo 1994; Hasselmo 1995; Liljenström and Hasselmo 1995). Likewise, serotonin (Colino and Halliwell 1987; Davies et al. 1987) and nora-drenaline (Madison and Nicoll 1982; 1986) have been shown to affect firing rate adaptation. In contrast, extrasynaptic release of GABA increases activation of potassium currents (Saint et al. 1990; Gage 1992). Consequently g_{KNa} increases during the transition into NREM sleep and declines during REM and wakefulness, see Table 1 for an overview. As there are no quantitative measurements, our choice of the dependency between the neuromodulator concentrations and g_{KNa} is arbitrary. For the sake of simplicity, we assume the following relationship for the strength of firing rate adaptation

$$\tau_g \dot{g}_{KNa} = \bar{g}_{KNa}(1 - 0.95C_A)(1 - 0.6C_E)(2C_G) - g_{KNa}. \quad (11)$$

The neural gain, on the other hand, is increased by acetylcholine (Barkai and Hasselmo 1994; Disney et al. 2007; Gullledge et al. 2009; Soma and Shimegi 2016), serotonin (Zhang and Arsenault 2005), and noradrenalin (McCormick 1989; Timmons et al. 2004). With σ_p acting as the inverse gain, it is maximal during NREM sleep and at the lowest during REM and wakefulness (see Table 1). Due to the lack of quantitative measurements which might hint to a more complex dependency, we work with the most simple assumption, namely a linear dependency between σ_p and the neuromodulator concentrations

$$\tau_\sigma \dot{\sigma}_p = \bar{\sigma}_p - (4C_E + 2C_A) - \sigma_p. \quad (12)$$

Computational methods The model was implemented in C++ and run within MATLAB R2015a, using a stochastic Runge-Kutta method of 4th order (Rößler 2010) with a step size of 0.1ms. The code is available at github (Schellenberger Costa 2006a). Each simulation had a duration of 24h with an initial onset of 10 seconds until recording. Background noise was given as white noise with zero mean and a standard deviation of $\phi_n^{sd} = 2\text{ms}^{-1}$. Symbol descriptions and parameter values are given in Tables 2, 3, 4 and 5.

Table 1 Neuromodulators and bifurcation parameters

| | Wake | NREM | REM |
|------------------------|------|------|------------|
| Acetylcholine | low | low | high |
| Noradrenalin/Serotonin | high | low | increasing |
| extrasynaptic GABA | low | high | high |
| g_{KNa} | low | high | low |
| σ_p | low | high | low |

Qualitative levels of neuromodulators and their influence on the bifurcation parameters

3 Results

3.1 Sleep regulation

Here, we will recapitulate our results in comparison to the reduced Diniz Behn model and relate them to changes of the bifurcation parameters of the cortex model. As illustrated in Fig. 3, the system is primarily in a state of wakefulness, accompanied by high levels of noradrenalin, during which the homeostatic sleep drive increases. Given sufficiently large sleep pressure the cortex will then transition into NREM sleep, characterized by elevated levels of GABA. As can be seen in Fig. 2 the NREM population also inhibits REM sleep. However, inhibition through GABA is weaker than that by noradrenalin during wakefulness ($|g_{GR}| > |g_{ER}|$), which leads to a slow increase in REM activity that ultimately switches the system into REM sleep.

The high levels of acetylcholine during REM sleep promote release of noradrenalin. As noradrenalin suppresses the REM population, REM sleep is terminated through reciprocal interaction between the Wake and the REM population. The ultradian cycling between NREM and REM sleep continues until the homeostatic sleep drive is sufficiently low. At that point the Wake population takes over and the system transitions from REM sleep to wakefulness. Following Diniz Behn and Booth wakefulness is defined as

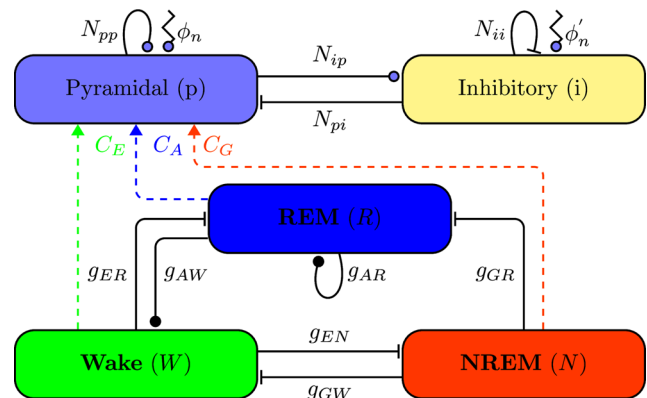


Fig. 2 Connectivity within the model. In the cortical submodule one pyramidal (p) and one inhibitory (i) population are all-to-all coupled, with connection strength N_{kl} where k denotes the postsynaptic and l the presynaptic population. Circles indicate excitatory and butts inhibitory synaptic input. Background activity from other unspecified brain areas modulates cortical activity through noisy inputs ϕ_n and ϕ'_n . The sleep regulatory network consists of three populations, Wake (W), NREM (N), and REM (R), that are associated with a specific neuromodulator, which is noradrenalin (E) for Wake, acetylcholine (A) for REM, and GABA (G) for the NREM population. They interact mainly through inhibition, with the interaction strength given by the synaptic weights g . The sleep regulatory network modulates activity of the pyramidal population through the respective neuromodulators C . The different types of neuromodulatory input are indicated by colored triangles connected through dashed lines

states with $C_E > 0.4$, REM through $C_A > 0.4$, and all other states as NREM. As described below, we utilize the activity of the cortical model to score the different sleep stages similar to experimental sleep research.

Due to its simplicity the presented sleep regulatory network exhibits differences with regard to human sleep EEG. In the model, the ultradian rhythm is uniform over the night, with equal portions of NREM and REM sleep for every cycle. This is in contrast to human sleep EEG, where NREM sleep is dominant in the first half of the night, whereas REM sleep occupies the better part of the second half. In the chosen 3 population regulatory network, the duration of REM episodes is directly linked to those of NREM through the reciprocal interaction with the Wake population. Initiation of REM sleep is due to declining levels of noradrenalin during NREM, whereas termination of REM is driven by increasing levels of noradrenalin (Fig. 3). Therefore, prolonging a REM episode would also lead to a longer NREM stage.

Furthermore, as there is only one NREM population, the model is not able to capture the deepening of NREM sleep within an ultradian cycle, which can be observed in the human EEG. This is exemplified in the lower panel of the Fig. 3, where the classification of sleep stages is based

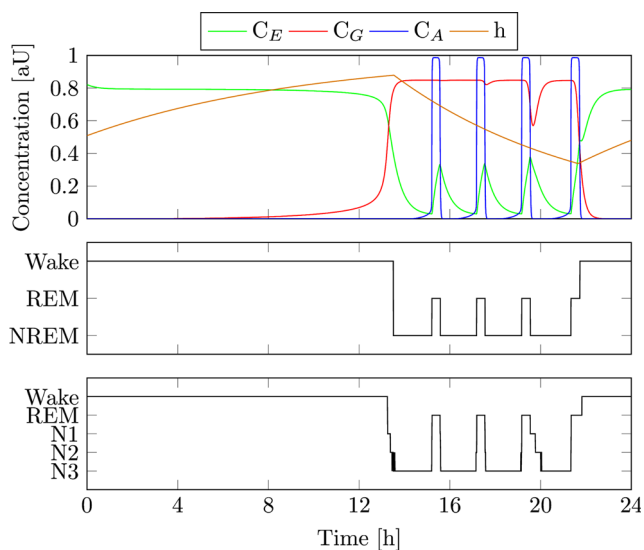


Fig. 3 Activity of the sleep regulatory network. In the upper panel the concentration of the different neurotransmitters in the sleep regulatory network is shown over the course of one day, together with the homeostatic sleep drive. The concentrations are directly related to the firing rates of the different populations. In the mid panel the hypnogram according to Diniz Behn and Booth (Diniz Behn and Booth 2012) is shown, which is based on the activity of the sleep regulatory network. In contrast, the lower panel depicts the hypnogram based on scoring of the activity of the pyramidal population, following the AASM rules for the EEG. There, we further subdivide NREM sleep into stages N1–N3

on the activity of the cortex. Except for the last ultradian cycle, where the NREM population shows a distinct drop in activity, the transition into sleep stage N3 is nearly instant, whereas in human sleep, N2 occupies a majority of NREM sleep (Fig. 1 for comparison). Interestingly the last ultradian cycle shows a prolonged transition from N1 over N2 to finally sleep stage N3. This is due to reduced sleep pressure h , that results in a reduced activity of the NREM population. Here a more sophisticated model, where NREM promoting populations are silenced during REM sleep might lead to more realistic results.

3.2 Modulation of the bifurcation parameters

As discussed above, the varying levels of neuromodulators affect the two bifurcation parameters g_{KNa} and σ_p . The combination of the three different neuromodulators leads to an increase of both parameters during NREM sleep and a decline during REM and wakefulness (See Fig. 4). Given the slow timescale of the sleep regulatory network, the bifurcation parameters can be assumed as quasi-static, so that our findings on the isolated cortex (Weigenand et al. 2014) are still valid for the coupled system and we can use the same bifurcation diagram.

During wakefulness the model is close to the z-axis around $\sigma_p = 4$ and $g_{KNa}=0$, which corresponds to a parameter configuration of the wake state given by a similar model of Steyn-Ross et al. (2005). During the transitions into NREM sleep, declining levels of noradrenaline lead to an increase in σ_p and g_{KNa} . At the same time GABA activates potassium channels, increasing g_{KNa} . When the

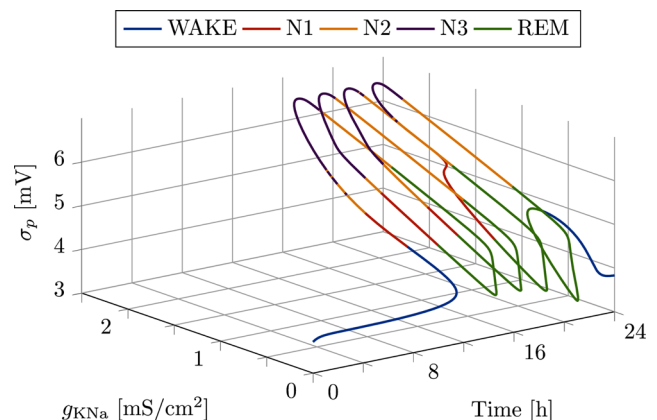


Fig. 4 Trajectory of the bifurcation parameters. The figure illustrates the time course of the two bifurcation parameters, modulated by the sleep regulatory network. To better relate the change of the bifurcation parameters to the activity of the cortical populations, the trajectory is color coded with respect to the scored sleep stage. During NREM sleep, both g_{KNa} and σ_p increase, to drop again during REM sleep. Over the night, the system undergoes four ultradian cycles, with the last cycle being strongly influenced by the drop in NREM activity

model switches into REM sleep, rising levels of acetylcholine rapidly decrease the adaptation strength g_{KNa} . In addition, neural gain is increased by acetylcholine and noreadrenalin, leading to smaller values of σ_p . Over the night the ultradian cycle is repeated multiple times (See Fig. 5).

However, there are notable differences between the respective ultradian cycles, that are not reflected in the classification of Diniz Behn and Booth. Especially during the last cycle, the activity of the NREM populations is significantly decreased after the REM episode (See Fig. 5). Importantly, this leads to a different trajectory in the bifurcation diagram of the cortex model, that directly affects the dynamics of the cortical populations, resulting in a different scoring in the EEG based hypnogram in Fig. 3. Due to decreased levels of GABA, the firing rate adaptation g_{KNa} recovers slowly. This puts the cortex in a trajectory farther away from the Hopf bifurcation, where it is unable to generate a canard explosion, leading to a prolonged period of N1. This puts the cortex in a trajectory farther away from the Hopf bifurcation, where it is unable to generate a canard explosion, leading to a prolonged period of N1.

In the wake state, the cortex is far away from the Hopf bifurcation in a single active state. When the homeostatic sleep drive intensifies, the NREM population activates. This leads to an release of extrasynaptic GABA and the cortex approaches the Hopf bifurcation as both g_{KNa} and σ_p increase (See Fig. 6 red line). As NREM sleep deepens further, the canard vanishes in a cusp bifurcation, with only the limit cycle of the Hopf bifurcation remaining. At the onset of REM sleep, rising levels of acetylcholine block firing rate adaptation through g_{KNa} , pushing the cortex away

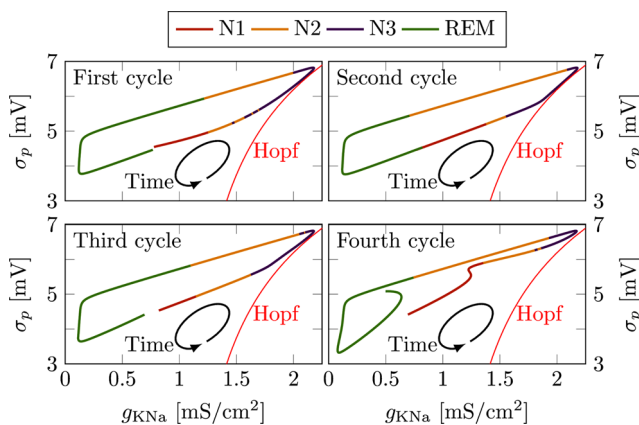


Fig. 5 Trajectory of the ultradian cycles. The panels depict the four ultradian cycles, the model fulfills during a night. Notably, the last ultradian cycle differs considerably from the others, as it is influenced by reduced NREM activity. This leads to a slower increase in g_{KNa} . The resulting trajectory is farther away from the Hopf bifurcation leading to a prolonged period of N1 and a slower transition phase into slow wave sleep (N3). As indicated the time flows counterclockwise

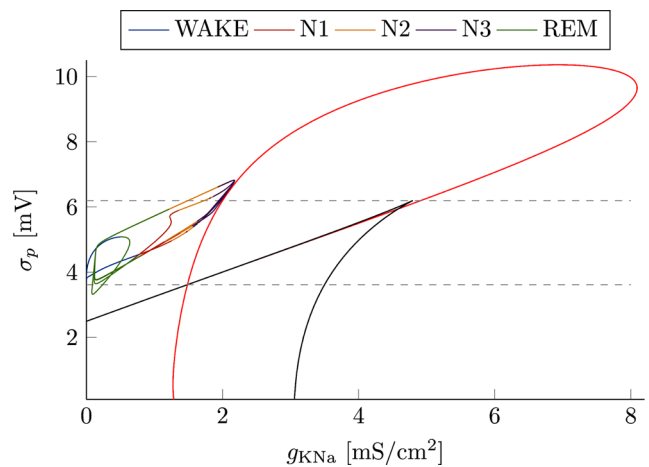


Fig. 6 Trajectory in the bifurcation diagram. This figure depicts, the projection of the time course of the bifurcation parameters onto the bifurcation diagram from Weigenand et al. (2014). Here, the red line denotes Hopf bifurcations, whereas the black line stands for saddle nodes. The trajectory of the cortex model is color coded with respect to the classification of the sleep stages. With the cortex moving closer to the Hopf bifurcation, the high frequency oscillations during wakefulness turn into low frequency large amplitude oscillations. During REM sleep increasing concentrations of acetylcholine push the model back to the lower left leading to higher frequency oscillations. It should be noted, that the projection does not reflect the time spend at the given point

from the Hopf bifurcation. Without its influence, the model returns to high frequency oscillations generated by synaptic interactions.

3.3 Effect of sleep regulation on the EEG

Cortical activity modulated by the sleep regulatory network is shown in Fig. 7. In the wake state, the cortex is in a depolarized stable equilibrium. Without influence of the Hopf bifurcation synaptic interactions dominate and it generates the typical high frequency low amplitude oscillations observed in the EEG during the day (Fig. 8-Wake).

During the early part of the wake-sleep transition, the system is increasingly affected by the ghost of the homoclinic orbit generated by the Hopf bifurcation. After perturbations through the background noise, the system does not directly return to the equilibrium, but follows a trajectory that is shaped by the homoclinic orbit. This results in a slow down in oscillation frequency and an increase in amplitude, corresponding to sleep stage N1 (Fig. 8-N1).

As sleep deepens further, the cortex moves closer to the Hopf bifurcation, where a canard phenomenon (Benoit et al. 1981) emerges through the interaction between the fast cortical activity and the slow firing rate adaptation. Importantly, the low frequency background oscillations may be interrupted by large amplitude deflections, which resemble

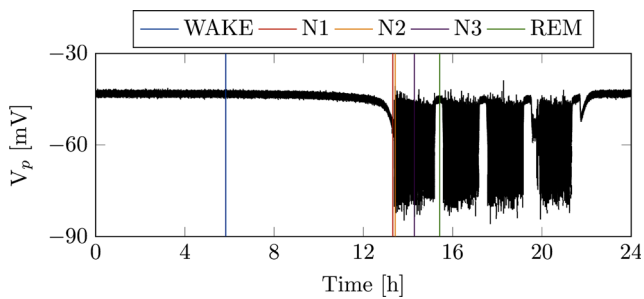


Fig. 7 Modulation of cortical activity over the day. Here, we illustrate the effect of modulation by the sleep regulatory network on the activity of the cortical model represented by the averaged membrane voltage of the pyramidal population V_p . After a period of wakefulness, the model transitions into NREM sleep, characterized by large amplitude oscillations. NREM episodes are interrupted by REM sleep, that resembles wakefulness. After 4 cycles of the ultradian rhythm, the cortex returns to a state of wakefulness. The vertical lines indicate the position of the respective episodes depicted in Fig. 8

K-complexes. They are initiated by background noise that pushes the system into the attractor of the canard, resulting in a single canard cycle around the silent hyperpolarized state (Fig. 6-N2).

With increasing σ_p the canard vanishes in a cusp bifurcation (marked by the upper dotted line in Fig. 6) and only a limit cycle remains. The previously isolated K-complexes are replaced by continuous noise driven large amplitude oscillations which resemble slow oscillatory activity during sleep stage N3 (Fig. 8-N3). Importantly, at no time the system actually crosses the Hopf bifurcation, but rather approaches it. Otherwise the highly regular limit cycle oscillations would generate pathologically seizure behavior.

When the sleep regulatory network switches to REM sleep, the increasing levels of acetylcholine push the cortex away from the Hopf bifurcation. Without its influence the cortex returns to low amplitude high frequency oscillations which are typical for REM sleep (Fig. 8-REM). The transition between the different sleep stages is depicted in Fig. 9. It occurs rapidly as close proximity to the limit cycle is necessary for slow wave activity, and blockage of g_{KNa} through acetylcholine moves the system perpendicularly to the Hopf bifurcation (Fig. 6).

3.4 Transition between sleep stages

In human sleep research, the classification into different sleep stages is based on electrophysiological measurements. However, in the Diniz Behn and Booth model as well as the related literature, there is no correlate of such activity. Here, we can directly relate the EEG signal generated by the activity in the cortical model to the ongoing activity in the sleep regulatory network. Therewith, we can provide a classification that directly relates activity of the sleep

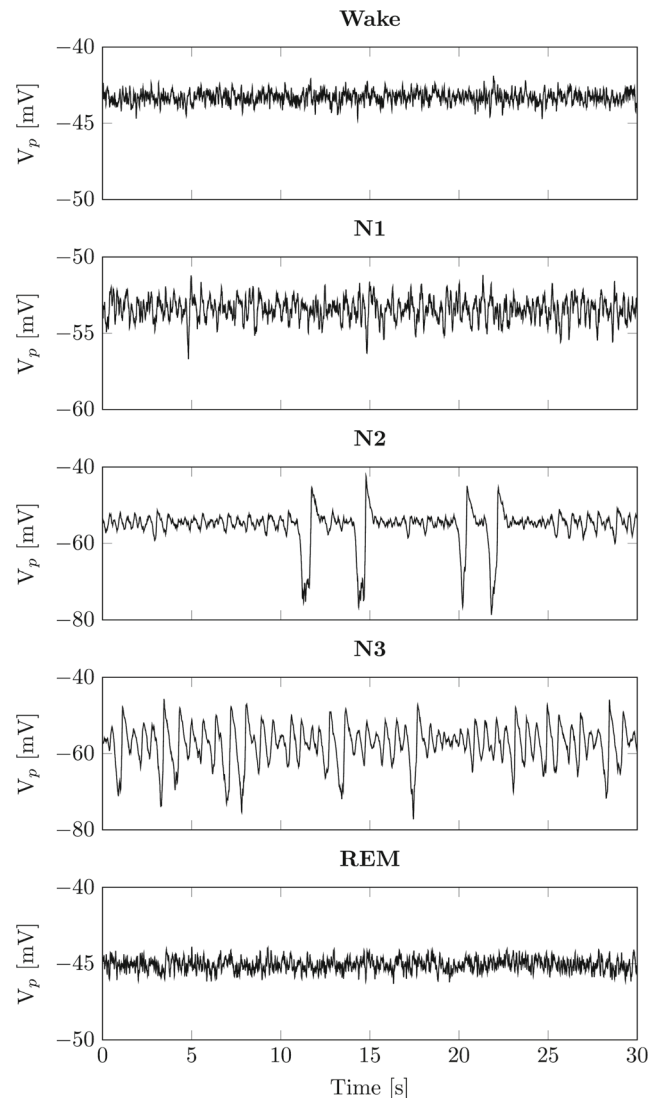


Fig. 8 Individual sleep stages generated by the model. The individual panels depict example epochs from Fig. 7, that correspond to different sleep stages following the classification scheme by the AASM (Iber et al. 2007). Activity during REM sleep resembles wakefulness, with the exception, that the cortex is relatively hyperpolarized. The panels N1-N3 show NREM sleep of increasing depth, with K-complexes emerging during N2 and slow wave activity during N3. Please note the different scales of the y axis especially for N2 and N3

regulatory network to experimental measurements. We follow the more recent classification scheme provided by the American Academy of Sleep Medicine (AASM) (Iber et al. 2007), although the classical rules by Rechtschaffen and Kales (1968) would apply equally. It should be noted, that our classification is solely based on the EEG part of the manual, as our model cannot generate EOG or EMG activity. The sleep scoring based on the activity of the pyramidal population is shown in Fig. 3.

The transitions between the different sleep stages are heavily dependent on two sets of time scales. The first are the time scales of neurotransmitter release in the sleep

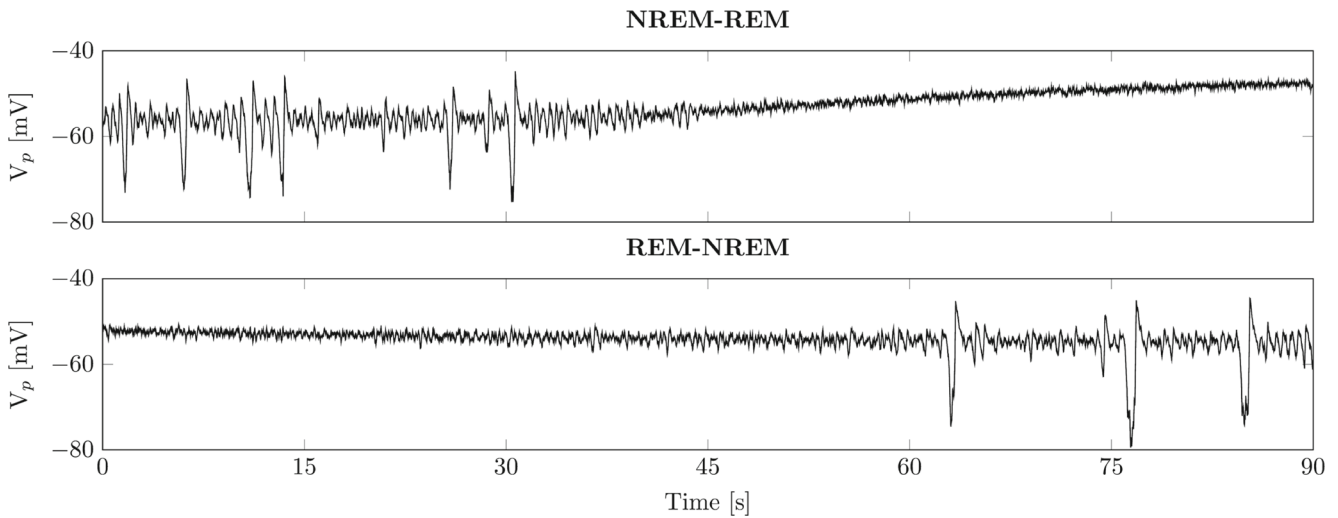


Fig. 9 Transition between sleep stages. This figure demonstrates the ability of the cortex model to rapidly switch between NREM and REM sleep. During NREM the cortex is close to the Hopf bifurcation leading to low frequency large amplitude oscillations. When the system transits into REM sleep, the increasing levels of acetylcholine block potassium

channels, pushing the cortex away from the Hopf. Immediately the slow oscillatory activity vanishes and gives rise to high frequency low amplitude oscillations typical for REM sleep. For brevity the transition between wakefulness and NREM sleep is omitted, as it is identical to the REM-NREM transition

regulatory network, τ_E , τ_G , and τ_A respectively. They are directly related to the intrinsic dynamics of the sleep regulatory network. Given the large timescales the sleep regulatory populations act upon, the behavior of the model is more sensitive to changes in τ_X than to changes in cortical timescales. The larger the time constants, the slower the transition between the different sleep stages.

The other set are the time constants of the bifurcation parameters τ_g and τ_σ in Eqs. (11) and (12) respectively. Here, we assume them to be in the range of tens to hundreds of milliseconds, which yielded the best results. It might be difficult to directly measure them *in vivo*, as they cover rather unspecific processes, e.g. neuronal gain is affected by many neuromodulators which might have different time scales individually. For the sake of simplicity we have also assumed that activation and inactivation of neuromodulators has the same time constant.

Importantly the two time constants τ_g and τ_σ cover different aspects of the sleep transitions. The change in firing rate adaptation g_{KNa} is crucial for the generation of large amplitude oscillations, as its axis is mostly orthogonal to the line of Hopf points. Therefore, τ_g has a strong influence on the ability of the model to rapidly switch into and out of NREM sleep, which is depicted in Fig. 9.

In contrast, changes in σ_p move the system on a trajectory parallel to the Hopf bifurcation. Therefore, it does not determine *whether* the cortex is able to generate large amplitude oscillations, but rather if they are generated through a canard explosion or through a limit cycle. Therefore, τ_σ mainly affects the speed, the system transitions from early NREM sleep (N2) to late NREM sleep (N3). However, as

sleep is scored in epochs of 30s, physiological values of τ_σ have only a minimal effect on the hypnogram (data not shown). To effectively change the distribution between N2 and N3, τ_σ would have to be in the range of minutes to hours, which suggests that the lack of N2 is not of cortical origin.

Note, that τ_g and τ_σ cannot be chosen arbitrarily, as the line of Hopf points is not fully parallel to the σ_p axis. Therefore, if τ_σ is sufficiently large compared to τ_g , the cortex might cross the Hopf bifurcation at a smaller g_{KNa} and generate unrealistic limit cycle oscillations.

4 Discussion

In this study we combined two different yet related modeling frameworks. On the one hand sleep regulatory networks and their complex interactions, that govern the transition between different states of vigilance. On the other hand EEG generating models, with a special emphasize on sleep. We utilized the modulatory effect of the neurotransmitters released by the sleep regulatory network, e.g. noradrenalin, GABA, and acetylcholine, on key parameters of the cortical neural mass model to regulate the transition between its different dynamics modes.

4.1 Neuromodulators and bifurcation parameters

A key aspect of this work is the modulation of the bifurcation parameters of the cortical model through the sleep regulatory network. We have shown, that the combined

model is able to generate key patterns observed in the EEG over a full day, independently from external input. While physiological studies provide a very clear grand picture of the qualitative effect the neuromodulators have on the different parameters (see Table 1), the literature lacks quantitative measurements of these changes. Therefore, we choose a simple dependency between g_{KNa} , σ_p , and the neuromodulators as a starting point for Eqs. (11) and (12). Here, neurophysiological measurements might help to elucidate the dependency of those bifurcation parameters on the respective neuromodulators and provide a better fit of their relationship.

4.2 Distribution of NREM and REM sleep

In the original model from Diniz Behn and Booth (2012), the NREM and REM episodes are uniformly distributed over the duration of the night. This is in contrast to human sleep data, where NREM sleep occupies the majority of the first half of the night and vice versa. Inclusion of the circadian rhythm through activity in the SCN has been shown to introduce a distribution of the REM bout durations (Fleshner et al. 2011; Gleit et al. 2013). However, this increases the complexity of the sleep regulatory network significantly. Also the reduction to a single REM population with reciprocal interactions might be critical, as other mechanisms beyond reciprocal interaction have been hypothesized to be involved in REM sleep regulation (Brown et al. 2008; Lu et al. 2006; Luppi et al. 2006; Sapin et al. 2009), which are also subject to circadian modulation. This requires more detailed models of both the REM sleep regulation as well as the circadian rhythm to elucidate the mechanisms underlying the distribution of REM sleep.

It is also possible to scale the strength of REM sleep related weights g_{ER} and g_{AW} in the sleep regulatory network with the homeostatic sleep drive h , to prolong REM episodes over the night (data not shown). However, given the high level of simplification in the chosen sleep regulatory model, it is questionable whether there is a physiological process corresponding to this scaling. The aim of this study is to provide a minimal physiologically plausible model of sleep regulation in a neural mass model. Therefore, we believe that rather than fixing minor aspects of an oversimplified sleep regulatory network, one should relate to more sophisticated models, e.g. (Rempe et al. 2009; Diniz Behn and Booth 2010; Kumar et al. 2012).

4.3 Subdivision of NREM sleep

Currently the literature on sleep regulatory network focuses on two cardinal rhythms, the sleep-wake transition as well

as NREM-REM cycling. However, in human sleep there is a further subdivision of NREM sleep into the sleep stages N1-N3, which corresponds to increasing depth of sleep and are characterized by unique features in the EEG. While our model can generate EEG activity that shows the characteristics of all stages of NREM sleep (See Fig. 8), N1 and N2 only appear as transients during the transition to sleep stage N3. In human sleep, N1 occupies only a minimal fraction of the night and is indeed assumed transient, whereas N2 accounts for the majority of sleep.

The small influence the timescales of the bifurcation parameters have on the hypnogram suggests that it is not possible to represent both N2 and N3 by a single population to fully reproduce human sleep EEG. Here, more sophisticated models, that include the subdivision of NREM sleep into two distinct sleep stages N2 and N3, will be necessary to fully capture sleep dynamics. Similar to REM sleep, the distribution of NREM varies over the night. This includes not only the total amount of NREM compared to REM, but also the distribution between N2 and N3. Modulation by the circadian rhythm might also play a crucial role, as changes in REM bout duration also affect NREM distribution.

Finally, the assumption, that all neuromodulators manipulate the bifurcation parameters on the same time scale might not be valid and those different time scales might play an important role in the transition between the different sleep stages.

4.4 Outlook

Our approach provides a direct relation between the activity of a sleep regulatory network and a generating model of human EEG. As sleep regulation affects the cortical model only indirectly through a slow modulation of the bifurcation parameters, the sleep regulatory network can be replaced by a different one, making it a useful tool for validating other sleep regulatory models.

Similar to the estimation of effective connectivity in the dynamic causal modeling framework (Kiebel et al. 2008), the EEG signal generated by the cortical model can be utilized to infer a mapping from human EEG data to the bifurcation parameters and therewith levels of neuromodulators. As this translates to the activity of the sleep regulatory network, it provides insights into activity of regulatory networks that otherwise might not be easily measured *in vivo*. This might allow the investigation of sleep related pathological conditions e.g. narcolepsy.

In addition to pathological conditions, our model can provide predictions for neuropharmacological interventions that either target the bifurcation parameters or neuromodulators, e.g. the model suggests that the application of

a cholinergic antagonist during REM sleep should lead to the emergence of slow oscillatory activity. Furthermore, anesthetic agents and neuromodulators have similar targets (Nicoll et al. 1990; Patel et al. 1999; Talley and Bayliss 2002), which could be incorporated in our model as an additional way of modifying the bifurcation parameters.

Acknowledgments We thank Arne Weigenand, Hong-Viet V. Ngo, Lisa Marshall, and Matthias Mölle for valuable discussions.

Appendix

A Model equations

The cortex model is given by the following set of equations:

$$\begin{aligned} \tau_p \dot{V}_p &= -I_L^p - I_{\text{AMPA}}(s_{ep}) - I_{\text{GABA}}(s_{gp}) - \tau_p C_m^{-1} I_{\text{KNa}}, \\ \tau_i \dot{V}_i &= -I_L^i - I_{\text{AMPA}}(s_{ei}) - I_{\text{GABA}}(s_{gi}), \\ \ddot{s}_{ep} &= \gamma_e^2 (N_{pp} Q_p(V_p) + \phi_n - s_{ep}) - 2\gamma_e \dot{s}_{ep}, \\ \ddot{s}_{gp} &= \gamma_g^2 (N_{pi} Q_i(V_i) - s_{gp}) - 2\gamma_g \dot{s}_{gp}, \\ \ddot{s}_{ei} &= \gamma_e^2 (N_{ip} Q_p(V_p) + \phi'_n - s_{ei}) - 2\gamma_e \dot{s}_{ei}, \\ \ddot{s}_{gi} &= \gamma_g^2 (N_{ii} Q_i(V_i) - s_{gi}) - 2\gamma_g \dot{s}_{gi}, \\ [\dot{\text{Na}}] &= (\alpha_{\text{Na}} Q_p(V_p) - N_{\text{apump}}([\text{Na}])) / \tau_{\text{Na}}, \\ \tau_g \dot{g}_{\text{KNa}} &= \bar{g}_{\text{KNa}}(1 - 0.95C_A)(1 - 0.75C_E)(1 + 0.85C_G) - g_{\text{KNa}}, \\ \tau_\sigma \dot{\sigma}_p &= \bar{\sigma}_p - (4C_E + 2C_A) - \sigma_p. \end{aligned}$$

With the currents defined by:

$$\begin{aligned} I_L &= \bar{g}_L (V_k - E_L), \\ I_{\text{AMPA}} &= \bar{g}_{\text{AMPA}} s_{ek} (V_k - E_{\text{AMPA}}), \\ I_{\text{GABA}} &= \bar{g}_{\text{GABA}} s_{gk} (V_k - E_{\text{GABA}}), \\ I_{\text{KNa}} &= g_{\text{KNa}} w_{\text{KNa}} (V_p - E_{\text{K}}), \\ w_{\text{KNa}} &= \frac{0.37}{1 + \left(\frac{38.7}{[\text{Na}]}\right)^{3.5}}. \end{aligned}$$

The sodium pump and firing rate functions are given by:

$$\begin{aligned} N_{\text{apump}}([\text{Na}]) &= R_{\text{pump}} \left(\frac{[\text{Na}]^3}{[\text{Na}]^3 + 3375} - \frac{[\text{Na}]_{\text{eq}}^3}{[\text{Na}]_{\text{eq}}^3 + 3375} \right), \\ Q_k(V_k) &= \frac{Q_k^{\text{max}}}{1 + \exp(-(V_k - \theta_k) / \sigma_k)}, \\ Q_k^{\text{SR}}(Y) &= \frac{F_k^{\text{max}}}{1 + \exp(-(Y - \beta_k) / \alpha_k)}. \end{aligned}$$

The sleep regulatory network is described by:

$$\begin{aligned} \tau_W \dot{F}_W &= Q_W (g_{GW} C_G + g_{AW} C_A) - F_W, \\ \tau_N \dot{F}_N &= Q_N (g_{EN} C_N) - F_N, \\ \tau_R \dot{F}_R &= Q_R (g_{ER} C_E + g_{GR} C_G + g_{AR} C_A) - F_R, \\ \tau_E \dot{C}_E &= \tanh(F_W / \gamma_E) - C_E, \\ \tau_G \dot{C}_G &= \tanh(F_N / \gamma_G) - C_G, \\ \tau_A \dot{C}_A &= \tanh(F_R / \gamma_A) - C_A, \\ \dot{h} &= \frac{h^{\text{max}} - h}{\tau_h^w} \mathcal{H}(F_W - \theta_h) - \frac{h}{\tau_h^s} \mathcal{H}(\theta_h - F_W). \end{aligned}$$

B Parameter values

Here, we describe the different symbols used in the cortex and sleep regulation module and give their values.

It should be noted, that in the original manuscript by Diniz Behn and Both the parameter values for the sleep regulatory network are given in seconds or hours. However, since we combine the cortical and the sleep regulatory model, we have to decide on one time unit.

Table 2 Symbol description cortex

| | |
|----------------------|--|
| C_m | Membrane capacitance in the HH model |
| Q_k^{max} | Maximal firing rate of population k |
| θ_k | Firing threshold of population k (half activation) |
| σ_k | Default gain coefficient of the firing rate function of population k (inverse neural gain) |
| τ_k | Membrane time constant of population k |
| τ_σ | Time constant of neural gain modulation |
| τ_g | Time constant of the modulation of the firing rate adaptation |
| γ_m | Synaptic rate constant of synapse type m |
| N_{kl} | Connectivity constant for presynaptic population l to postsynaptic population k |
| \bar{g}_X | Conductivity of channel X |
| E_X | Nernst reversal potential of channel X |
| α_{Na} | Sodium influx through firing rate |
| τ_{Na} | Time constant of sodium extrusion |
| R_{pump} | Strength of the sodium pump |
| N_{aeq} | Resting state sodium equilibrium |
| ϕ^{sd} | Standard deviation of background noise |

Table 3 Symbol description sleep regulation

| | |
|--------------|---|
| τ_K | Membrane time constant of population K |
| τ_X | Membrane time constant of neuromodulator X |
| F_K^{\max} | Maximal firing rate of population K |
| β_K | Firing threshold of population K (Half activation) |
| α_K | Default gain coefficient of the firing rate function of population K (neural gain). |
| γ_X | Synaptic rate constant of neuromodulator X |
| g_{XK} | Synaptic weight of neuromodulator X acting on postsynaptic population K |
| h^{\max} | Maximal sleep drive |
| θ_h | Sleep drive threshold |
| τ_h^w | Time constant of sleep drive build up during wakefulness |
| τ_h^s | Time constant of sleep drive decline during sleep |
| κ | NREM firing threshold modulation parameter |

Table 4 Parameter values cortex model

| Symbol | Value | Unit |
|-------------------------|----------------------|---------------------------|
| C_m | 1 | $\mu\text{F}/\text{cm}^2$ |
| τ_p, τ_i | 30 | ms |
| Q_p^{\max} | $30 \cdot 10^{-3}$ | ms^{-1} |
| Q_i^{\max} | $60 \cdot 10^{-3}$ | ms^{-1} |
| θ_p, θ_i | -58.5 | mV |
| $\bar{\sigma}_p$ | 7 | mV |
| $\bar{\sigma}_i$ | 6 | mV |
| τ_σ | 100 | ms |
| γ_e | $70 \cdot 10^{-3}$ | ms^{-1} |
| γ_g | $58.6 \cdot 10^{-3}$ | ms^{-1} |
| N_{pp} | 120 | – |
| N_{ip} | 72 | – |
| N_{pi} | 90 | – |
| N_{ii} | 90 | – |
| \bar{g}_L | 1 | – |
| \bar{g}_{AMPA} | 1 | ms |
| \bar{g}_{GABA} | 1 | ms |
| E_L^p | -66 | mV |
| E_L^i | -64 | mV |
| E_K | -100 | mV |
| E_{AMPA} | 0 | mV |
| E_{GABA} | -70 | mV |
| \bar{g}_{KNa} | 1.33 | mS/cm^2 |
| τ_g | 10 | ms |
| α_{Na} | 2 | $\text{mM}/\text{mA ms}$ |
| τ_{Na} | 1.7 | ms |
| R_{pump} | 0.09 | mM ms^{-1} |
| Na_{eq} | 9.5 | mM |
| ϕ_n^{sd} | 2 | ms^{-1} |

Table 5 Parameter values sleep regulation

| Symbol | Value | Unit |
|--------------|---------------------|------------------|
| τ_W | $1500 \cdot 10^3$ | ms |
| τ_N | $600 \cdot 10^3$ | ms |
| τ_R | $60 \cdot 10^3$ | ms |
| τ_E | $2.5 \cdot 10^3$ | ms |
| τ_G | $1 \cdot 10^3$ | ms |
| τ_A | $1 \cdot 10^3$ | ms |
| F_W^{\max} | $6.5 \cdot 10^{-3}$ | ms^{-1} |
| F_N^{\max} | $5 \cdot 10^{-3}$ | ms^{-1} |
| F_R^{\max} | $5 \cdot 10^{-3}$ | ms^{-1} |
| β_W | -0.4 | ms^{-1} |
| β_R | -0.9 | ms^{-1} |
| α_W | 0.5 | ms^{-1} |
| α_N | 0.175 | ms^{-1} |
| α_R | 0.13 | ms^{-1} |
| γ_E | $5 \cdot 10^{-3}$ | ms^{-1} |
| γ_G | $4 \cdot 10^{-3}$ | ms^{-1} |
| γ_A | $2 \cdot 10^{-3}$ | ms^{-1} |
| g_{GW} | -1.68 | – |
| g_{AW} | 1 | – |
| g_{GR} | -1.3 | – |
| g_{AR} | 1.6 | – |
| g_{ER} | -4 | – |
| g_{EN} | -2 | – |
| h^{\max} | 1 | – |
| θ_h | $2 \cdot 10^{-3}$ | ms^{-1} |
| τ_h^w | $34830 \cdot 10^3$ | ms |
| τ_h^s | $30600 \cdot 10^3$ | ms |
| κ | 1.5 | – |

References

- Atay, F.M., & Hutt, A. (2006). Neural fields with distributed transmission speeds and long range feedback delays. *SIAM Journal on Applied Dynamical Systems*, 5(4), 670–698. doi:10.1137/050629367.
- Barkai, E., & Hasselmo, M.E. (1994). Modulation of the input/output function of rat piriform cortex pyramidal cells. *Journal of Neurophysiology*, 72(2), 644–658.
- Benita, J.M., Guillamon, A., Deco, G., & Sanchez-Vives, M.V. (2012). Synaptic depression and slow oscillatory activity in a biophysical network model of the cerebral cortex. *Frontiers in computational neuroscience*, 6(64). doi:10.3389/fncom.2012.00064.
- Benoit, E., Callot, J.L., Diener, F., & Diener, M. (1981). Chasse au canard. *Collectanea Mathematica*, 31-32(1-3), 37–119.
- Booth, V., & Diniz Behn, C.G. (2014). Physiologically-based modeling of sleep-wake regulatory networks. *Mathematical Biosciences*, 250(1), 54–68. doi:10.1016/j.mbs.2014.01.012.
- Borbély, A.A. (1982). A two process model of sleep regulation Human neurobiology.
- Brown, R.E., McKenna, J.T., Winston, S., Basheer, R., Yanagawa, Y., Thakkar, M.M., & McCarley, R.W. (2008). Characterization

- of GABAergic neurons in rapid-eye-movement sleep controlling regions of the brainstem reticular formation in GAD67-green fluorescent protein knock-in mice. *European Journal of Neuroscience*, 27(2), 352–363. doi:10.1111/j.1460-9568.2008.06024.x.
- Colino, A., & Halliwell, J.V. (1987). Differential modulation of three separate K-conductances in hippocampal CA1 neurons by serotonin. *Nature*, 328(6125), 73–7. doi:10.1038/328073a0.
- Compte, A., Sanchez-Vives, M.V., McCormick, D.A., & Wang, X.J. (2003). Cellular and network mechanisms of slow oscillatory activity (<1Hz) and wave propagations in a cortical network model. *Journal of Neurophysiology*, 89(5), 2707–25. doi:10.1152/jn.00845.2002.
- Coombes, S. (2005). Waves, bumps, and patterns in neural field theories. *Biological Cybernetics*, 93(2), 91–108. doi:10.1007/s00422-005-0574-y.
- Daan, S., Beersma, D.G.M., & Borbély, A.A. (1984). Timing of human sleep: recovery process gated by a circadian pacemaker. *The American Journal of Physiology*, 246(2 Pt 2), 161–183.
- Datta, S., & MacLean, R.R. (2007). Neurobiological Mechanisms for the Regulation of Mammalian Sleep-Wake Behavior: Reinterpretation of Historical Evidence and Inclusion of Contemporary Cellular and Molecular Evidence. *Neuroscience Biobehavior Reviews*, 31(5), 775–824. doi:10.1016/j.biotechadv.2011.08.021.Secreted.
- David, O., & Friston, K.J. (2003). A neural mass model for MEG/EEG: coupling and neuronal dynamics. *NeuroImage*, 20(3), 1743–1755. doi:10.1016/j.neuroimage.2003.07.015.
- Davies, M.F., Deisz, R.A., Prince, D.A., & Peroutka, S.J. (1987). Two distinct effects of 5-hydroxytryptamine on single cortical neurons. *Brain Research*, 423(1-2), 347–52. doi:10.1016/0006-8993(87)90861-4.
- Deco, G., Jirsa, V.K., Robinson, P.A., Breakspear, M., & Friston, K.J. (2008). The dynamic brain: from spiking neurons to neural masses and cortical fields. *PLoS Computational Biology*, 4(8), e1000092. doi:10.1371/journal.pcbi.1000092.
- Deco, G., Martí, D., & Ledberg, A. (2009). Effective reduced diffusion-models: a data driven approach to the analysis of neuronal dynamics. *PLoS Computational Biology*, 5(12), e1000587. doi:10.1371/journal.pcbi.1000587.
- Diniz Behn, C.G., & Booth, V. (2010). Simulating microinjection experiments in a novel model of the rat sleep-wake regulatory network. *Journal of Neurophysiology*, 103(4), 1937–1953. doi:10.1152/jn.00795.2009.
- Diniz Behn, C.G., & Booth, V. (2012). A fast-slow analysis of the dynamics of REM sleep. *SIAM Journal on Applied Dynamical Systems*, 11(1), 212–242. doi:10.1137/110832823.
- Diniz Behn, C.G., Brown, E.N., Scammell, T.E., & Kopell, N.J. (2007). Mathematical model of network dynamics governing mouse sleep wake behavior. *Journal of Neurophysiology*, 97, 3828–3840. doi:10.1152/jn.01184.2006.
- Disney, A.A., Aoki, C., & Hawken, M.J. (2007). Gain modulation by nicotine in macaque v1. *Neuron*, 56, 701–713. doi:10.1016/j.neuron.2007.09.034.
- Fleshner, M., Booth, V., Forger, D.B., & Diniz Behn, C.G. (2011). Circadian regulation of sleep-wake behaviour in nocturnal rats requires multiple signals from suprachiasmatic nucleus. *Philosophical Transactions of the Royal Society A: Mathematical, physical, and engineering sciences*, 369(1952), 3855–3883. doi:10.1098/rsta.2011.0085.
- Forger, D.B., Jewett, M.E., & Kronauer, R.E. (1999). A simpler model of the human circadian pacemaker. *Journal of Biological Rhythms*, 14(6), 532–537. doi:10.1177/074873099129000867.
- Fuller, P.M., Saper, C.B., & Lu, J. (2007). The pontine REM switch: past and present. *The Journal of physiology*, 584(Pt 3), 735–741. doi:10.1113/jphysiol.2007.140160.
- Gage, P.W. (1992). Activation and modulation of neuronal K⁺ channels by GABA. *Trends in neurosciences*, 15(2), 46–51. doi:10.1016/0166-2236(92)90025-4.
- Gleit, R.D., Diniz Behn, C.G., & Booth, V. (2013). Modeling interindividual differences in spontaneous internal desynchrony patterns. *Journal of Biological Rhythms*, 28(5), 339–55. doi:10.1177/0748730413504277.
- Gulledge, A.T., Bucci, D.J., Zhang, S.S., Matsui, M., & Yeh, H.H. (2009). M1 receptors mediate cholinergic modulation of excitability in neocortical pyramidal neurons. *The Journal of Neuroscience*, 29(31), 9888–9902. doi:10.1523/JNEUROSCI.1366-09.2009.
- Hasselmo, M.E. (1995). Neuromodulation and cortical function: modeling the physiological basis of behavior. *Behavioural Brain Research*, 67(1), 1–27.
- Iber, C., Ancoli-Israel, S., Chesson Jr., A.L., & Quan, S.F. (2007). The AASM Manual for the Scoring of Sleep and Associated Events: Rules Terminology and Technical Specifications 1st ed.
- Jansen, B.H., Zouridakis, G., & Brandt, M.E. (1993). A neurophysiologically-based mathematical model of flash visual evoked potentials. *Electrical Engineering*, 283, 275–283.
- Kales, A., & Rechtschaffen, A. (1968). Rechtschaffen, A.: A manual of standardized terminology, techniques and scoring system for sleep stages of human subjects. U. S. National Institute of Neurological Diseases and Blindness, Neurological Information Network.
- Kiebel, S.J., Garrido, M.I., Moran, R.J., & Friston, K.J. (2008). Dynamic causal modelling for EEG and MEG. *Cognitive Neurodynamics*, 2(2), 121–136. doi:10.1007/s11571-008-9038-0.
- Kumar, R., Bose, A., & Mallick, B.N. (2012). A mathematical model towards understanding the mechanism of neuronal regulation of wake-NREMS-REMS states. *PLoS One*, 7(8), 1–17. doi:10.1371/journal.pone.0042059.
- Léna, I., Parrot, S., Deschaux, O., Muffat-Joly, S., Sauvinet, V., Renaud, B., Suaud-Chagny, M.F., & Gottesmann, C. (2005). Variations in extracellular levels of dopamine, noradrenaline, glutamate, and aspartate across the sleep-wake cycle in the medial prefrontal cortex and nucleus accumbens of freely moving rats. *Journal of Neuroscience Research*, 81(6), 891–899. doi:10.1002/jnr.20602.
- Liljeström, N., & Hasselmo, M.E. (1995). Cholinergic modulation of cortical oscillatory dynamics. *Journal of Neurophysiology*, 74(1), 288–297.
- Lopes da Silva, F.H., Hoeks, A., Smits, H., & Zetterberg, L.H. (1974). Model of brain rhythmic activity. The alpha-rhythm of the thalamus. *Kybernetik*, 15(1), 27–37.
- Lu, J., Sherman, D., Devor, M., & Saper, C.B. (2006). A putative flip-flop switch for control of REM sleep. *Nature*, 441(7093), 589–594. doi:10.1038/nature04767.
- Luppi, P.H., Gervasoni, D., Verret, L., Goutagny, R., Peyron, C., Salvert, D., Leger, L., & Fort, P. (2006). Paradoxical (REM) sleep genesis: The switch from an aminergic-cholinergic to a GABAergic-glutamatergic hypothesis. *Journal of Physiology Paris*, 100(5-6), 271–283. doi:10.1016/j.jphysparis.2007.05.006.
- Lydic, R., & Baghdoyan, H.A. (2005). Sleep, anesthesiology, and the neurobiology of arousal state control. *Anesthesiology*, 103(6), 1268–1295. doi:10.1097/0000542-200512010-00024.
- Madison, D.V., & Nicoll, R.A. (1982). Noradrenaline blocks accommodation of pyramidal cell discharge in the hippocampus. *Nature*, 299, 636–638. doi:10.1038/299636a0.
- Madison, D.V., & Nicoll, R.A. (1986). Actions of noradrenaline recorded intracellularly in rat hippocampal CA1 pyramidal neurons, *in vitro*. *The Journal of Physiology*, 372, 221–244.
- Madison, D.V., Lancaster, B., & Nicoll, R.A. (1987). Voltage clamp analysis of cholinergic action in the hippocampus. *The Journal of Neuroscience*, 7(3), 733–741.

- Marreiros, A.C., Daunizeau, J., Kiebel, S.J., & Friston, K.J. (2008). Population dynamics: Variance and the sigmoid activation function. *NeuroImage*, 42, 147–157. doi:10.1016/j.neuroimage.2008.04.239.
- McCarley, R.W., & Hobson, J.A. (1975). Neuronal excitability modulation over the sleep cycle: a structural and mathematical model. *Science*, 189(4196), 58–60. doi:10.1126/science.1135627.
- McCormick, D.A. (1989). Cholinergic and noradrenergic modulation of thalamocortical processing. *Trends in Neurosciences*, 12(6), 215–221. doi:10.1016/0166-2236(89)90125-2.
- McCormick, D.A., & Huguenard, J.R. (1992). A model of the electrophysiological properties of thalamocortical relay neurons. *Journal of Neurophysiology*, 68(4), 1384–400.
- Moruzzi, G. (1972). The sleep-waking cycle. *Ergebnisse der Physiologie, biologischen Chemie und experimentellen Pharmakologie*, 64, 1–165.
- Nicoll, R.A., Malenka, R.C., & Kauer, J.A. (1990). Functional comparison of neurotransmitter receptor subtypes in mammalian central nervous system. *Physiological Reviews*, 70(2), 513–565.
- Patel, A.J., Honoré, E., Lesage, F., Fink, M., Romey, G., & Lazdunski, M. (1999). Inhalational anesthetics activate two-pore-domain background K⁺ channels. *Nature Neuroscience*, 2(5), 422–426. doi:10.1038/8084.
- Peyron, C., Tighe, D.K., Van den Pol, A.N., de Lecea, L., Heller, H.C., Sutcliffe, J.G., & Kilduff, T.S. (1998). Neurons containing hypocretin (orexin) project to multiple neuronal systems. *The Journal of Neuroscience*, 18(23), 9996–10.
- Phillips, A.J.K., & Robinson, P.A. (2007). A quantitative model of sleep-wake dynamics based on the physiology of the brainstem ascending arousal system. *Journal of Biological Rhythms*, 22(2), 167–179. doi:10.1177/0748730406297512.
- Rasch, B., & Born, J. (2013). About sleep's role in memory. *Physiological Reviews*, 93(2), 681–766. doi:10.1152/physrev.00032.2012.
- Rempe, M.J., Best, J., & Terman, D.H. (2009). A mathematical model of the sleep/wake cycle. *Journal of Mathematical Biology*, 60(5), 615–644. doi:10.1007/s00285-009-0276-5.
- Rößler, A. (2010). Runge-Kutta methods for the strong approximation of solutions of stochastic differential equations. *SIAM Journal on Numerical Analysis*, 48(3), 922–952. doi:10.1137/09076636X.
- Saint, D.A., Thomas, T., & Gage, P.W. (1990). GABAB agonists modulate a transient potassium current in cultured mammalian hippocampal neurons. *Neuroscience Letters*, 118(1), 9–13. doi:10.1016/0304-3940(90)90236-3.
- Sanchez-Vives, M.V., & McCormick, D.A. (2000). Cellular and network mechanisms of rhythmic recurrent activity in neocortex. *Nature Neuroscience*, 3(10), 1027–34. doi:10.1038/79848.
- Saper, C.B., Chou, T.C., & Scammell, T.E. (2001). The sleep switch: Hypothalamic control of sleep and wakefulness. *Trends in Neurosciences*, 24(12), 726–731. doi:10.1016/S0166-2236(00)02002-6.
- Saper, C.B., Scammell, T.E., & Lu, J. (2005). Hypothalamic regulation of sleep and circadian rhythms. *Nature*, 437(7063), 1257–1263. doi:10.1038/nature04284.
- Sapin, E., Lapray, D., Béro, A., Goutagny, R., Léger, L., Ravassard, P., Clément, O., Hanriot, L., Fort, P., & Luppi, P.H. (2009). Localization of the brainstem GABAergic neurons controlling Paradoxical (REM) sleep. *PLoS One*, 4(1). doi:10.1371/journal.pone.0004272.
- Schellenberger Costa, M. (2006a). Simulation routine of the model. <https://github.com/miscco/NM.Cortex.SR>.
- Soma, S., & Shimegi, S. (2016). Cholinergic modulation of response gain in the primary visual cortex of the macaque. *Journal of Neurophysiology*, 107, 283–291. doi:10.1152/jn.00330.2011.
- Steyn-Ross, D.A., Steyn-Ross, M.L., Sleigh, J.W., Wilson, M.T., Gillies, I.P., & Wright, J.J. (2005). The sleep cycle modelled as a cortical phase transition. *Journal of Biological Physics*, 31(3–4), 547–569. doi:10.1007/s10867-005-1285-2.
- Talley, E.M., & Bayliss, D.A. (2002). Modulation of TASK-1 (Kcnk3) and TASK-3 (Kcnk9) potassium channels volatile anesthetics and neurotransmitters share a molecular site of action. *Journal of Biological Chemistry*, 277(20), 17,733–17,742. doi:10.1074/jbc.M200502200.
- Tamakawa, Y., Karashima, A., Koyama, Y., Katayama, N., & Nakao, M. (2006). A quartet neural system model orchestrating sleep and wakefulness mechanisms. *Journal of Neurophysiology*, 95(4), 2055–2069. doi:10.1152/jn.00575.2005.
- Timmons, D., Geisert, E., Stewart, E., Lorenzon, M., & Foehring, R.C. (2004). Alpha 2-Adrenergic receptor-mediated modulation of calcium current in neocortical pyramidal neurons. *Brain Research*, 1014, 184–196. doi:10.1016/j.brainres.2004.04.025.
- Weigenand, A., Schellenberger Costa, M., Ngo, H.V.V., Claussen, J.C., & Martinetz, T. (2014). Characterization of K-complexes and slow wave activity in a neural mass model. *PLoS Computational Biology*, 10, e1003,923. doi:10.1371/journal.pcbi.1003923.
- Wendling, F., Bartolomei, F., Bellanger, J.J.J., & Chauvel, P. (2002). Epileptic fast activity can be explained by a model of impaired GABAergic dendritic inhibition. *European Journal of Neuroscience*, 15(9), 1499–1508. doi:10.1046/j.1460-9568.2002.01985.x.
- Wilson, H.R., & Cowan, J.D. (1973). A mathematical theory of the functional dynamics of cortical and thalamic nervous tissue. *Kybernetik*, 13(2), 55–80.
- Zhang, Z.W., & Arsenault, D. (2005). Gain modulation by serotonin in pyramidal neurones of the rat prefrontal cortex. *The Journal of Physiology*, 2, 379–394. doi:10.1113/jphysiol.2005.086066.